The Highly Preorganized Ligand PDA (1,10-Phenanthroline-2,9-dicarboxylic Acid) for the Selective Recovery of Uranium from Seawater in the Presence of Competing Vanadium Species

Mark A. Lashley,[§#] Alexander S. Ivanov,[ǂ#] Vyacheslav S. Bryantsev,[*ǂ] Sheng Dai,[ǂ] and Robert D. Hancock[*§]

[§]Department of Chemistry and Biochemistry, University of North Carolina Wilmington, Wilmington, North Carolina 28403, United States

[ǂ]Oak Ridge National Laboratory, Chemical Sciences Division, 1 Bethel Valley Road, Oak Ridge, Tennessee 37831-6119, United States

Supporting Information

ABSTRACT: Studies of the complexation of new promising ligands with uranyl (UO_2^{2+}) and other seawater cations can aid the development of more efficient, selective, and robust sorbents for the recovery of uranium from seawater. In this work, we propose that the ligand design principles based on structural preorganization can be successfully applied to obtain a dramatic enhancement in UO_2^{2+} ion binding affinity and selectivity. This concept is exemplified through the investigation of the complexes of UO_2^{2+}, VO_2^{+}, and VO^{2+} with the highly preorganized ligand PDA (1,10-phenanthroline-2,9-dicarboxylic acid) using a combination of fluorescence and absorbance techniques, along with density functional theory (DFT) calculations. The measured stability constant value, log K_1, of 16.5 for the UO_2^{2+}/PDA complex is very high compared to uranyl complexes with other dicarboxylic ligands. Moreover, PDA exhibits strong selectivity for uranyl over vanadium ions, since the determined stability constant values of the PDA complexes of the vanadium ions are quite low (V(IV) log K_1 = 7.4, V(V) = 7.3). The structures of the corresponding UO_2^{2+}, VO_2^{+}, and VO^{2+} complexes with PDA were identified by systematic DFT calculations, and helped to interpret the stronger binding affinity for uranium over the vanadium ions. Due to its high chemical stability, selectivity, and structural preorganization for UO_2^{2+} complexation, PDA is a very promising candidate that can be potentially used in the development of novel adsorbent materials for the selective extraction of uranium from seawater.

INTRODUCTION

In a comment article recently published in the journal *Nature*, the extraction of uranium from seawater was listed among seven energy-intensive separation processes that would “change the world” providing new routes to the resources that people need.[1] Indeed, there is at present considerable interest in recovering uranium from the oceans.[2-6] While the known uranium reserves on land can sustain power generation for about a century at the current consumption rates, more than 4.5 x 10^9 tons of uranium is dissolved in the world’s oceans, affording almost limitless supply of uranium for the nuclear fuel cycle.[7] Since the concentration of uranium in seawater is very low (1.3 x 10^{-8} M),[7] functional groups of substantial binding strengths are needed to extract uranium, and to overcome competition from the carbonate ligand present in seawater at a relatively high concentration of 2.5 x 10^{-3} M.[8] Currently, the leading approach for extraction of uranium from seawater is the sorption of uranyl ions, UO_2^{2+}, onto a poly(acrylamidoxime) adsorbent.[9] This sorbent material contains polyethylene or polypropylene as a trunk polymer and amidoximated polyacrylonitrile copolymerized with hydrophilic groups (*e.g.*, acrylic, methacrylic, itaconic acids) as a graft chain (Scheme 1). Although amidoxime ligands exhibit high uranyl binding affinity,[10,11] they have the drawback of low selectivity over other cations in seawater.[12] In particular, vanadium ions, present in the oceans as pentavalent VO_2^{+} and tetravalent VO^{2+} species at total concentrations of about 4.0 x

10^{-8} M,[13-15] are significantly absorbed by poly(acrylamidoxime) fibers, diminishing the effective sites that are available for uranium and thus significantly reducing the sorption capacity and efficiency. Furthermore, the vanadium species bind so strongly that stripping them under harsh acidic conditions irreversibly damages the amidoxime sorbent.[6,16] Therefore, to improve the performance of fiber adsorbents to its maximum, ligands should have low binding affinity for competing cations such as vanadium, and at the same time very high binding affinity for uranyl in the slightly basic (pH = ~8.3) marine environment. It is known that the addition of acidic co-monomers increases the sorption capacity of the sorbent by improving the hydrophilicity of the fiber. For instance, adsorbents with the weight ratio of amidoxime/carboxylic acid = 60/40 in the monomer mixture have been reported to exhibit the highest uranium adsorption rate.[17] However, hydrophilic adsorbent fibers containing 100% of mono- and dicarboxylic acid groups are not expected to show high uranium uptake, because carboxylates are typically weak Lewis bases, and should not form strong complexes with UO_2^{2+}, which is a strong Lewis acid metal. Nevertheless, uranyl complexing properties of carboxylates can be significantly enhanced *via* ligand design principles based on structural preorganization,[18,19] which is the focus of the present study.

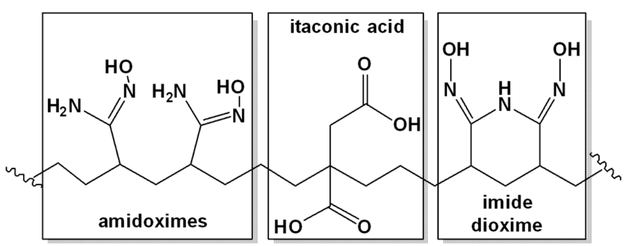

Scheme 1. Schematic depiction of a small subsection of the poly(acrylamidoxime) fiber.

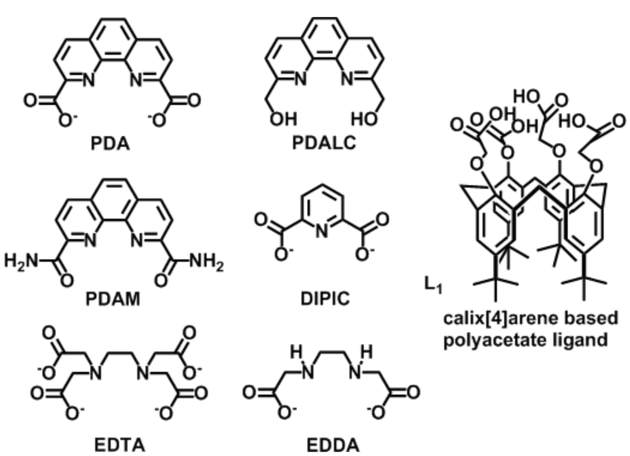

Figure 1. Ligands discussed in this paper.

In 1987 Shinkai et al.[20] applied the principles of rational ligand design to the calixarene-based ligand – uranyl system. Although strong extraction of uranyl by calixarenes (*e.g.* L_1 in Figure 1) with acetate groups arranged so that they would bind in the plane of the UO_2^{2+} has been achieved, metal ion selectivity appears again to be a problem.[20,21] The complexes of L_1 and its larger calix[5]arene and calix[6]arene analogues seem to have the highest known log K_1 values with UO_2^{2+} among the carboxylic-based ligands,[20] illustrating the capability of preorganization[18,19] to produce ligands of high complexing power. Thus, oxalate has a log β_3 with the UO_2^{2+} cation of only 11.0,[22] but the calix[6]arene-based analogue of L_1, also providing six carboxylate donor groups, forms a complex of UO_2^{2+} with log K_1 = 19.2.[20] Beer et al.[23] demonstrated successful extraction of UO_2^{2+} by three rigid 2,6-terphenyl acid ligands from aqueous solutions in the presence of excess brine. However, the appropriate association constants for the resulting complexes have not been measured. Another interesting example highlighting the importance of structural preorganization in the design of uranophiles was recently reported by Zhou et al.[24] It was shown that otherwise poor-coordinating natural amino acids were able to achieve the highest recorded uranium selectivity in seawater because they were preorganized within a protein to form an ideal binding site for the uranyl ion.[24]

We decided to test the highly preorganized ligand PDA (1,10-phenanthroline-2,9-dicarboxylic acid) (Figure 1), because it possesses a high complexing power.[25-27] The ligand forms three five-membered chelate rings upon complexation with large metal ions, having ionic radii (r^+) in the vicinity of 1.0 Å.[28,29] This is particularly important, as UO_2^{2+} is effectively a large metal ion, with in-plane bond lengths quite similar to those of lanthanum, La^{III}, with r^+ = 1.04 Å.[30] In contrast, the competing VO_2^+ and VO^{2+} ions are comparatively small, which should lead to much lower complex stability and result in higher selectivity for UO_2^{2+} over vanadium. The extensive preorganization of PDA is derived from the rigidity of the phenanthroline (phen) backbone, which also affords high levels of preorganization in analogues such as PDAM and PDALC.[31-37] The size-based selectivity increases as the denticity of the ligand increases from 2 in phen to 4 in DPP. This is displayed in Scheme 2 for selectivity of the large Cd^{II} ion (r^+ = 1.00 Å) over the small Zn^{II} ion (r^+ = 0.74 Å), or the large Ca^{II} ion (r^+ = 1.00 Å) over the small Mg^{II} ion (r^+ = 0.74 Å). What the data in Scheme 2 suggest is that log K_1 for a bidentate ligand is largely controlled by the affinity of the metal ion for the donor atoms, with little input from architectural effects such as chelate ring size. However, for the tetradentate ligand, the arc created by the four N donors causes severe steric difficulties for the small Zn^{II} and Mg^{II} ions, such that the crystal structure of the Zn^{II}/DPP complex (r^+ = 0.74 Å) shows that one of the pyridyl groups of DPP is not coordinated to the Zn^{II} at all, whereas with Cd^{II} (r^+ = 0.96 Å) all four N donors are coordinated.[36,37]

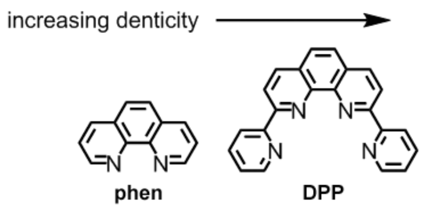

	phen	DPP
log K_1 Cd^{2+}: (large)	5.4	12.2
log K_1 Zn^{2+}: (small)	6.4	8.7
log K_1 Ca^{2+}: (large)	1.0	3.8
log K_1 Mg^{2+}: (small)	1.5	0.7

Scheme 2. The effect of increasing denticity in passing from phen to DPP on the selectivity of large metal ions over otherwise chemically similar small metal ions. Formation constant (log K_1) data from refs. 32 and 33.

The PDA ligand is tetradentate and like DPP highly preorganized, with all binding sites positioned to structurally complement the uranyl ion. The combined results of the spectroscopic and *ab initio* studies of the UO_2^{2+}/PDA complex reported here suggest that ligand preorganization plays a significant role in the enhanced uranyl binding affinity. The complex stability of the PDA complexes of VO_2^+ and VO^{2+} are also reported here, so as to allow for assessment of the probable selectivity of PDA-based ion exchange materials for UO_2^{2+} over these vanadium species. Since it is of interest to know how apparently small ions such as VO_2^+ and VO^{2+} as well as a large UO_2^{2+} ion coordinate with PDA in aqueous solution, density functional theory (DFT) calculations were performed to elucidate the optimal coordination modes and geometries of VO_2^+/PDA, VO^{2+}/PDA, and UO_2^{2+}/PDA complexes. In addition, stability constant values for UO_2^{2+}, VO_2^+, and VO^{2+} complexes with simple aliphatic dicarboxylic acids were theoretically assessed to trace how structural preorganization affects the ligand binding affinity and selectivity.

EXPERIMENTAL METHODS

Materials. PDA was synthesized by a literature method.[38] $UO_2(NO_3)_2$•$6H_2O$ (depleted) was obtained from Fisher and used without further purification. All solutions were prepared in deionized water (Milli-Q, Waters Corp.) of > 18 MΩ.cm^{-1} resistivity, plus HPLC grade methanol from Merck.

Fluorescence Measurements. Excitation-emission matrix (EEM) fluorescence properties were determined on a Jobin Yvon SPEX Fluoromax-3 scanning fluorometer equipped with a 150 W Xe arc lamp and a R928P detector. The instrument was configured to collect the signal in ratio mode with dark offset using 5 nm band-passes on both the excitation and emission monochromators. The EEMs were created by concatenating emission spectra measured every 5 nm from 250 to 500 nm at 51 separate excitation wavelengths. Scans were corrected for instrument configuration using factory supplied correction factors. The fluorescence of the PDA metal ion solutions was recorded in Milli-Q water, with titrations occurring in an external cell with N_2 bubbled through the cell to exclude O_2.

Absorbance spectra. UV-Visible spectra were recorded using a Varian 300 Cary 1E UV-Visible Spectrophotometer controlled by Cary Win UV Scan Application version 02.00(5) software. A VWR sympHony™ SR60IC pH meter with a VWR sympHony™ gel epoxy semi-micro combination pH electrode was used for all pH readings, which were made in the external titration cell, with N_2 bubbled through the cell to exclude CO_2. The absorbance spectra of the PDA metal ion solutions were recorded in Milli-Q water. Formation constant were determined using Excel.[39]

COMPUTATIONAL METHODS

Quantum chemical calculations. Electronic structure calculations were performed with the Gaussian 09 D.01 software.[40] We adopted the density functional theory (DFT) approach for our calculations using the M06[41] density functional with the standard Stuttgart small-core (SSC) 1997 relativistic effective core potential (RECP),[42] the associated contracted [6s/5p/3d/1f] and [8s/7p/6d/4f] basis sets for vanadium and uranium atoms, respectively, and the 6-311++G(d,p) basis set for the light atoms. Frequency calculations were performed at the B3LYP/SSC/6-31+G(d)[43] level to ensure that geometries (optimized at the same B3LYP/SSC/6-31+G(d) level) were minima and to compute zero-point energies and thermal corrections. Hindered rotation corrections for ligands with low frequency modes (e.g., the rotation of CH_3 and C_2H_5 groups along the C-C bond) were also incorporated in the complexation free energy calculations following the method of Pitzer and Gwinn[44] as implemented by Schlegel et al.[45]

Using the gas-phase geometries, implicit solvent corrections were obtained at 298 K with the SMD[46] solvation model as implemented in Gaussian 09 at the B3LYP/SSC/6-31+G(d) level of theory. The results are reported using the lowest energy clusters identified at the M06/SSC/6-311++G(d,p) level for a given stoichiometry and binding motif.

Optimized atomic coordinates for all reported structures, as well as a sample Gaussian 09 input file, are provided as Supporting Information.

The preference for using a combination of the M06 and the B3LYP functionals with the SMD solvation model was based on the results of our previous studies,[47-49] which showed that the chosen level of theory provides the best overall performance in predicting the log K_1 values of uranyl[47,48] and vanadium[49] ions complexes with anionic oxygen and amidoxime donor ligands.

Chemical bonding analysis of $[UO_2(PDA)(H_2O)]$, $[VO_2(PDA)(H_2O)]^-$, and $[VO(PDA)]$ complexes was performed with the natural bond orbital (NBO) method[50] at B3LYP/SSC/6-311++G(d,p) using NBO 6.0 program. It is worth noting that total electron densities derived from effective core potential (ECP) calculations may lead to artifacts in the topological analysis,[51] however, NBO derived properties appear to be less critical in this respect and showed a remarkable consistency between ECP and scalar relativistic all-electron calculation schemes,[52] thus justifying our choice towards ECP for the description of chemical bonding.

Calculation of the complexation free energies and stability constants. Complexation free energies in aqueous solution, ΔG_{aq}, and stability constants, log K_1, were calculated using the methodology described in our previous work on UO_2^{2+} as well as VO_2^+ and VO^{2+} containing complexes.[47-49] According to the thermodynamic cycle shown in **Scheme 3**, ΔG_{aq} is given by:

$$\Delta G_{aq} = \Delta G^o_g + \Delta\Delta G^*_{solv} + (n\text{-}1)\Delta G^{o\rightarrow *} + nRT\ln([H_2O])$$

where ΔG^o_g is the free energy of complexation in the gas phase and $\Delta\Delta G^*_{solv}$ is the difference in the solvation free energies for a complexation reaction:

$$\Delta\Delta G^*_{solv} = \Delta G^*_{solv}([ML(H_2O)_{m-n}]^{x+y}) + n\Delta G^*_{solv}(H_2O) - \Delta G^*_{solv}([M(H_2O)_m]^x) - \Delta G^*_{solv}(L^y)$$

where L^y denotes the ligand with a charge of y and M can be UO_2^{2+} or VO_2^+/VO^{2+}. The standard state correction terms must be introduced to connect ΔG^o_g, $\Delta\Delta G^*_{solv}$, and ΔG_{aq}, which are defined using different standard state conventions. The free energy change for the conversion of 1 mol of solute from the gas phase at a standard state of 1 atm (24.46 L/mol) to the aqueous phase at a standard state of 1 mol/L at 298.15 K is given by $\Delta G^{o\rightarrow *}$ = 1.89 kcal/mol. Likewise, $RT\ln([H_2O])$ = 2.38 kcal/mol (T = 298.15 K) is the free energy change for the conversion of 1 mol of solvent from the aqueous phase at 1 mol/L to pure water at a standard state of 55.34 mol/L. Lastly, the stability constant (log K_1) value is related to free energy change for the complexation reaction by the following equation:

$$\log K_1 = \frac{-\Delta G_{aq}}{2.303 \cdot RT}$$

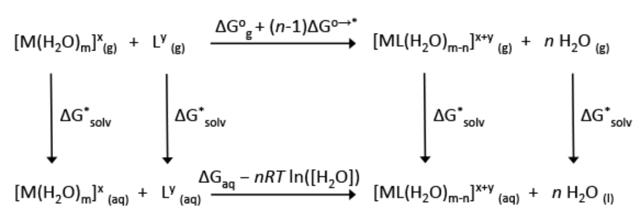

Scheme 3. Thermodynamic cycle used to calculate ΔG_{aq}.

RESULTS AND DISCUSSION

Stability Constants of UO_2^{2+}, VO_2^+, and VO^{2+} Complexes with Aliphatic Dicarboxylate Ligands.

As was mentioned in the introduction, the incorporation of acidic groups such as acrylate and itaconate into a poly(acrylamidoxime) adsorbent is crucial to obtain a high uranium uptake. Although hydrophilic carboxylate ligands have been suggested to help seawater to access the amidoxime groups on the graft chain,[17,53] the exact mechanism has not yet been fully established and understood.

According to some experimental[54] and theoretical[55] studies, carboxylic acid functional groups can also directly participate in binding with uranyl ions. In an effort to probe the dependence of the complexing properties of simple dicarboxylate ligands on the extent of their structural preorganization, we have assessed the stability constant, log K_1, values for the UO_2^{2+}, VO_2^+, and VO^{2+} complexes with oxalic, malonic, succinic, and glutaric acids. In contrast to the experimental data for the uranium complexes available in the Smith and Martell compilation of the Critical Stability Constants series,[22] the log K_1 values for the VO_2^+ and VO^{2+} complexes are available only for oxalic and malonic ligands. To supplement this lack of data, we have applied our recently developed approach[49] based on quantum chemical calculations to estimate and compare the equilibrium constants for the formation of VO_2^+ and VO^{2+} complexes with the aforementioned dicarboxylic ligands. The log K_1 values of the UO_2^{2+} complexes were also theoretically calculated to make sure that the adopted computational method is capable of reproducing experimental log K_1 data for the complexes with dicarboxylic ligands having a long alkyl chain. Since only the first coordination shell of the uranium and vanadium complexes was treated explicitly, it was possible to perform a systematic search of low-energy clusters for a given composition. The most stable geometries of the complexes were used to compute the corresponding free energies in aqueous solution, ΔG_{aq}, and stability constants, log K_1. According to our calculations, the dicarboxylic acids form stronger complexes with UO_2^{2+}, VO_2^+, and VO^{2+} ions through chelation involving both carboxylate functional groups. The results of the log K_1 calculations for the dicarboxylic ligands are summarized in Table 1.

Table 1. Experimental and Theoretically Calculated log K_1 Values for Uranyl, Dioxovanadium (V), and Oxovanadium (IV) Complexes with Dicarboxylate Ligands

ligand	log K_1					
	UO_2^{2+}		VO_2^+		VO^{2+}	
	expt[a]	calc[b]	expt[a]	calc[b]	expt[a]	calc[b]
I oxalate	7.3	6.6	6.6	5.6	7.0	6.0
II malonate	6.9	7.0	5.2	5.6	6.7	6.2
III succinate	5.2	4.9	-	6.8	-	5.4
IV glutarate	4.8	4.5	-	6.6	-	4.9
V itaconate	5.8[c]	5.1	-	6.7	-	5.3
VI 2,2-dimethylsuccinate	-	6.4	-	7.7	-	6.1

[a]Taken from ref. 21 and corrected to zero ionic strength with the Davies equation.[56] The corresponding experimental data for the VO_2^+ and VO^{2+} complexes with ligands III-VI are not available.
[b]Calculated using the methodology described in refs. 47,48 (UO_2^{2+} complexes) and ref. 49 (VO_2^+ and VO^{2+} complexes).
[c]Taken from ref. 57.

As one may see, our theoretical protocol provides a good estimate of the log K_1 values for the considered set of ligands, with the maximum absolute error below 1 log unit. In order to find the trend in the relative binding affinity and selectivity of the dicorboxylate ligands we have compared log K_1 values for the corresponding UO_2^{2+}, VO_2^+, and VO^{2+} complexes. A histogram of the calculated log K_1 values for the metal oxycation complexes as a function of the length of the ligand's aliphatic chain (Figure 2, ligands: I-IV) shows that more flexible ligands tend to form weaker complexes with UO_2^{2+} and VO^{2+} cations. However, the opposite trend is observed for the complexes with VO_2^+, suggesting that increasing the number of alkyl groups in the aliphatic chain can lead to a positive effect on the stability of the VO_2^+/dicarboxylate systems.

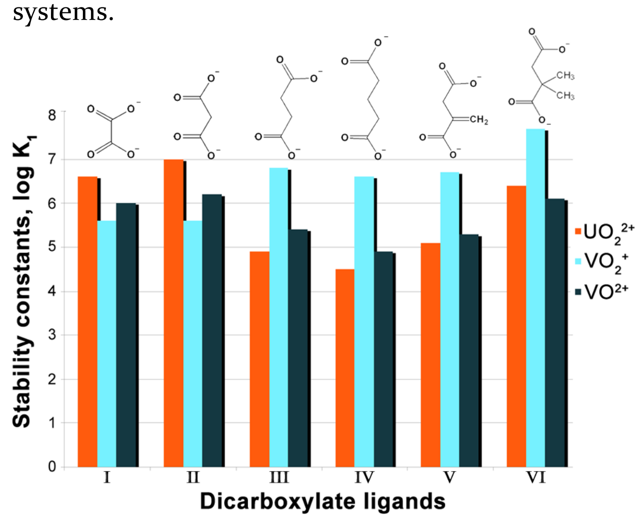

Figure 2. Comparison of theoretically predicted log K_1 values for UO_2^{2+} (red), VO_2^+ (turquoise), and VO^{2+} (dark blue) complexes with dicarboxylate ligands: I) oxalate, II) malonate, III) succinate, IV) glutarate, V) itaconate (2-methylenesuccinate), VI) 2,2-dimethylsuccinate.

The log K_1 values for the UO_2^{2+}, VO_2^+, and VO^{2+} complexes with itaconic acid (Figure 2, structure V) were also theoretically assessed (see Table 1). Itaconic acid, which contains a vinyl group connected directly to a succinic acid terminus, is often used as a co-monomer in the synthesis of poly(acrylamidoxime) adsorbents for the extraction of uranium from seawater. Since in the actual adsorbent the vinyl group is polymerized to give a branched polyethylene, aliphatic 2,2-dimethylsuccinic acid (Figure 2, structure VI) would be a more accurate model representation of itaconic acid grafted on a fiber. Theoretically predicted log K_1^{calc} value of the VO_2^+ complex with VI is 1.3 and 1.6 log units higher than that of the UO_2^{2+} and VO^{2+} complexes, respectively, indicating higher selectivity of VI towards VO_2^+ over UO_2^{2+} and VO^{2+} ions. Interestingly, recent experimental studies on the performance of poly(acrylamidoxime) adsorbent show higher vanadium uptake selectivity over uranium, irrespectively of grafting the adsorbent with different mole ratios of amidoxime and itaconic acid.[53] Overall, our results suggest that simple aliphatic dicarboxylic ligands possess low binding affinity and selectivity for uranyl, because their backbones present architectures that are poorly organized for the UO_2^{2+} complexation. Indeed, the two carboxyl groups of the lowest-energy conformers of the dycarboxylic acids point in opposite directions such that it is not possible for the two oxygen atoms to simultaneously contact the metal ion. Therefore, the dicarboxylate structure must adopt a higher-energy conformation to allow chelation. Our calculations show that in addition to the entropically disfavored restricted rotation about C-C bonds, the structural changes induced by metal chelation lead to increasing ligand strain, with a strain energy, ΔE_{reorg} (E_{bound} – E_{free}), of 39.50 kcal/mol (M06/SSC/6-311++G**) for the least preorganized glutarate ligand, which exhibits the smallest stability constant value with UO_2^{2+} (log K_1^{calc} = 4.5).

The foregoing analysis suggests that a considerable enhancement in binding affinity and selectivity for uranyl over vanadium ions can be achieved if the dycarboxylates are conformatially constrained in a favorable host architecture that is structurally organized for binding with UO_2^{2+}, thereby eliminating unfavorable entropic and enthalpic (strain energy) terms. For instance, dipicolinic acid, DIPIC (Figure 1), consisting of the rigid pyridine backbone that connects two carboxylic groups together, demonstrates a higher selectivity for UO_2^{2+} (log K_1^{expt} = 11.6) over VO_2^+ (log K_1^{expt} = 9.3) and VO^{2+} (log K_1^{expt} = 8.0) cations.[22] Thus, the incorporation of even more preorganized phenanthroline backbone is expected to result in much higher selectivity towards uranyl *versus* vanadium species.

Stability Constants of UO_2^{2+}, VO_2^+, and VO^{2+} Complexes with the Highly Preorganized PDA Ligand.

Uranyl/PDA complexes. The relatively low pK_a value of the PDA ligand and at the same time high log K_1 values found for PDA complexes[25-27] suggest that many of these complexes cannot be broken down by competition with the proton, even at pH values as low as 1.0. Many log K_1 values were determined by competition with EDTA,[25,27] but the low log K_1 for EDTA with UO_2^{2+} means that EDTA is unable to displace UO_2^{2+} from the UO_2^{2+}/PDA complex. Experimentation with the species distribution diagram program HySS[58] suggested that UO_2^{2+} would show amphoteric behavior at high pH values and low UO_2^{2+} concentrations, and is cleaved from the PDA ligand, suggesting that one might determine log K_1 for the UO_2^{2+}/PDA complex by competition with OH^-. The rather complex equilibria involving the UO_2^{2+}/OH^- species in solution have been extensively studied,[59-60] imparting confidence that these reported formation constants can be used reliably to measure log K_1 for the UO_2^{2+}/PDA complex.

The formation constant for the UO_2^{2+}/PDA complex was determined by monitoring both the fluorescence and absorbance spectra for 1:1 UO_2^{2+}:PDA solutions as a function of pH. In the case of the absorbance studies, spectra of solutions containing 1.0 x 10^{-5} M UO_2^{2+} and 1.0 x 10^{-5} M PDA were recorded over the pH range 2.0 - 12.5, and in the case of the fluorescence studies 5 x 10^{-5} M UO_2^{2+} and PDA solutions were used. Figure 3a displays the absorbance spectra for the 1:1 UO_2^{2+}:PDA solutions over the pH range 7-12. Fitting the theoretical curves showed that the pH dependent equilibrium around pH 11 involved two hydroxides. The limiting absorbance spectra of the species produced at pH values above 12 were those with peaks characteristic of the uncomplexed PDA^{2-} anion, while the spectra at around pH 10 showed peaks characteristic of a PDA metal ion complex. Based on the shape of the curve of fluorescence intensity versus pH and consistent with two hydroxides (or equivalently, two protons) involved in the equilibrium, the most reasonable interpretation of this equilibrium is as given in equation 1:

$$[UO_2(PDA)OH]^- + 2OH^- \leftrightarrows [UO_2(OH)_3]^- + PDA^{2-} \quad (1)$$

Theoretical curves of absorbance versus pH were fitted to the experimental data in Figure 3a. This produced a pH_{50} (pH at the midpoint of the curve of absorbance versus pH) of 11.52. Below a pH of 9 the UO_2^{2+}/PDA solutions began to show evidence of precipitate formation in terms of large light-scattering peaks in the wavelength region below 250 nm. Investigating the disappearance of the absorbance peaks due to the UO_2^{2+}/PDA complex as a function of time suggested that complete precipitation below pH 9 took approximately 3 hours. The fluorescence spectra appeared less sensitive to the formation of small amounts of precipitate, so that the variation of the fluorescence spectra as a function of pH was used to study the complex equilibria occurring below pH 9.

The fluorescence spectra of 5 x 10^{-5} M 1:1 PDA:UO_2^{2+} between pH 6 and 12.4 are seen in Figure 3b. The variation of fluorescence intensity versus pH at a variety of wavelengths was analyzed as seen in Figure 3c to yield a pH_{50} of 11.94 for the equilibrium apparent at higher pH. This is somewhat higher than the corresponding pH_{50} obtained from absorbance, which is typical of fluorescence studies.[62] The latter refer to the excited state, whereas absorbance and other techniques of determining formation constants refer to the ground state, and so can be somewhat different.[62] In Figure 3b further drops in pH reveal a second equilibrium best fitted as involving a single proton, which is found in Figure 3c to yield a pH_{50} of 8.77. This is most reasonably attributed to equilibrium (2), which yields a log *K* of 5.2 for the binding of an OH^- to the $[UO_2(PDA)]$ complex.

$$[UO_2(PDA)OH]^- + H^+ \leftrightarrows [UO_2(PDA)] + H_2O \qquad (2)$$

The two pH_{50} values can be combined in HySS[56] with all the equilibrium constants for formation of uranyl hydroxy complexes[59-61] to yield log K_1 = 16.5 for the uranyl PDA complex (Table 2), with the speciation as shown in Figure 3d.

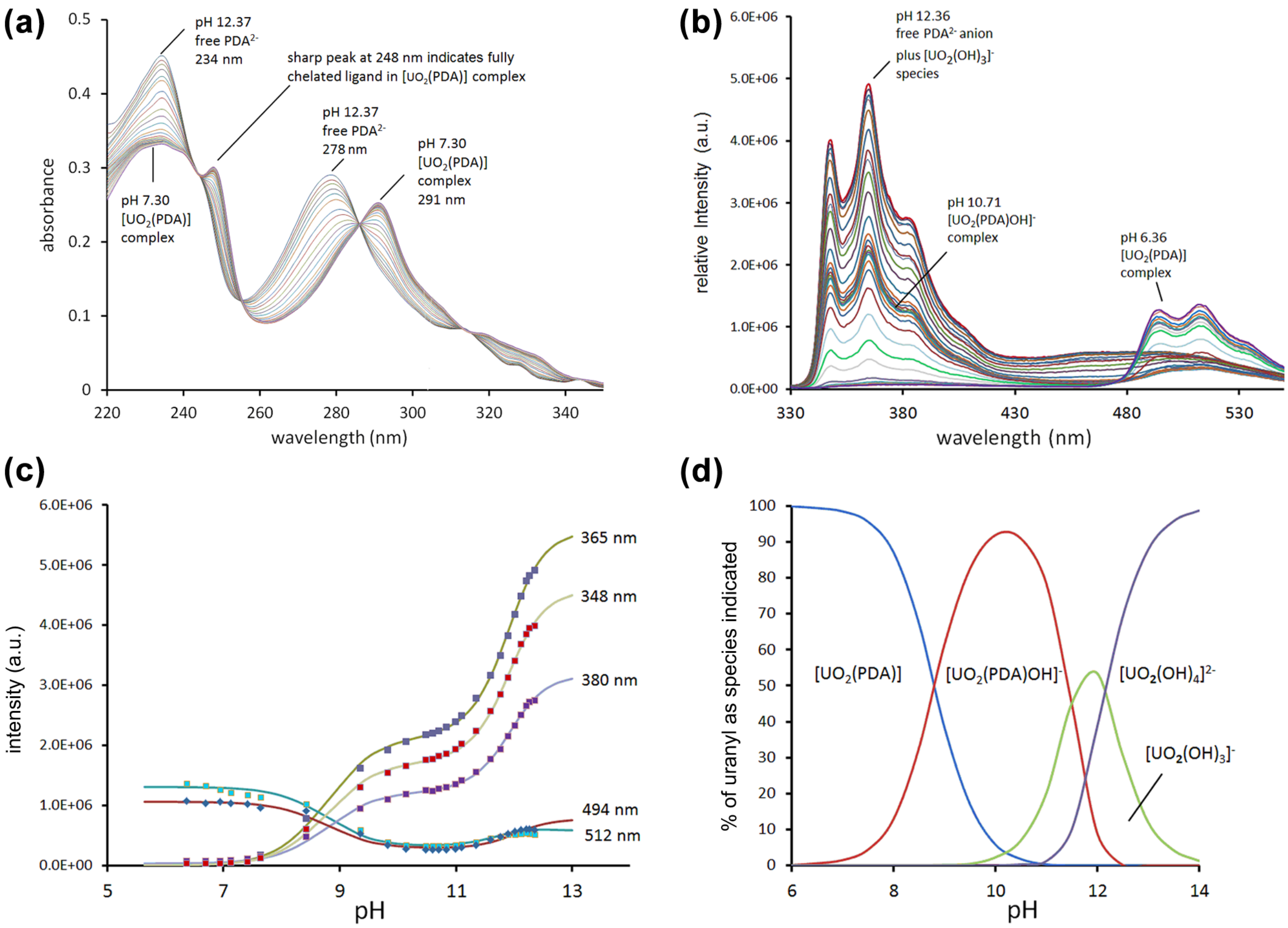

Figure 3. (a) Absorbance spectra of 1:1 solutions of PDA and UO_2^{2+} (as the nitrate), both 1.0 x 10^{-5} M, between pH 7.30 and 12.37. The sharp shoulder at 248 nm is considered to be diagnostic of fully coordinated PDA,[25] forming three chelate rings with the UO_2^{2+}, as seen in the crystal structure of the $[UO_2(PDA)]$ complex.[26] (b) Fluorescence spectra of 1:1 PDA:UO_2^{2+} solution (5 x 10^{-5} M) between pH 6.36 and 12.36. Excitation wavelength = 290 nm. (c) Variation of fluorescence intensity as a function of pH of 1:1 PDA:UO_2^{2+} solution (5 x 10^{-5} M) between pH 6.36 and 12.36.

Theoretical curves of fluorescence intensity as a function of pH were fitted using the Solver module of the Excel program. Excitation wavelength = 290 nm. (d) Species distribution diagram for 2 x 10^{-5} M UO_2^{2+} and 2 x 10^{-5} M PDA as a function of pH between pH 6 and 14. Diagram was calculated using HySS[58] and formation constants for uranyl-PDA complexes and uranyl hydroxy species given in Table 2.[22, 59-61]

Table 2. Equilibrium Constants for the UO_2^{2+}/PDA Complex, Together with Literature Constants for the Uranyl Hydroxo and Carbonato Complexes Used in This Work for Modeling Uranyl Solution Species, All at 25 °C and Ionic Strength (μ) = 0[22, 59-61]

equilibrium	log *K*	ref.
$H^+ + OH^- \leftrightarrows H_2O$	14.00	21
$H^+ + PDA^{2-} \leftrightarrows PDAH^-$	5.14(2)	this work*
$H^+ + PDAH^- \leftrightarrows PDAH_2$	2.80(2)	this work*
$UO_2^{2+} + PDA^{2-} \leftrightarrows UO_2(PDA)$	16.5(1)	this work
$UO_2(PDA) + OH^- \leftrightarrows UO_2(PDA)(OH)^-$	5.2(1)	this work
$UO_2^{2+} + OH^- \leftrightarrows UO_2(OH)^+$	8.75	57-59
$UO_2^{2+} + 2OH^- \leftrightarrows UO_2(OH)_2$	15.85	57-59
$UO_2^{2+} + 3OH^- \leftrightarrows UO_2(OH)_3^-$	21.8	57-59
$UO_2^{2+} + 4OH^- \leftrightarrows UO_2(OH)_4^{2-}$	23.6	57-59
$2UO_2^{2+} + OH^- \leftrightarrows (UO_2)_2(OH)^{3+}$	11.3	57-59
$2UO_2^{2+} + 2OH^- \leftrightarrows (UO_2)_2(OH)_2^{2+}$	22.4	57-59
$3UO_2^{2+} + 5OH^- \leftrightarrows (UO_2)_3O(OH)_3^+$	54.4	57-59
$3UO_2^{2+} + 7OH^- \leftrightarrows (UO_2)_3O(OH)_5^-$	65.3	57-59
$4UO_2^{2+} + 7OH^- \leftrightarrows (UO_2)_4O(OH)_5^+$	76.1	57-59
$UO_2^{2+} + 2OH^- \leftrightarrows (UO_2)(OH)_2(s)$	-22.0	21
$UO_2^{2+} + CO_3^{2-} \leftrightarrows UO_2(CO_3)$	9.68	57
$UO_2^{2+} + 2CO_3^{2-} \leftrightarrows UO_2(CO_3)_2$	16.9	57
$UO_2^{2+} + 3CO_3^{2-} \leftrightarrows UO_2(CO_3)_3$	21.6	57

*Previously reported at ionic strength = 0.1 as pK_1 = 4.75 and pK_2 = 2.53.[26]

Vanadate(V)/PDA complexes. The VO_2^+ cation has an extensive complex-formation chemistry in aqueous solution, forming complexes with ligands such as DIPIC and EDTA.[22] However, because of formation of species such as VO_4^{3-}, HVO_4^{2-}, and particularly $H_2VO_4^-$, which persists down to a pH of 3.5, below which pH the VO_2^+ cation is formed, only ligands powerful enough to displace the OH^- groups of $H_2VO_4^-$ to form complexes of the VO_2^+ cation will be observed at higher pH. In Figure 4a are shown absorbance spectra of 2 x 10^{-5} M Na_3VO_4 anion in the presence of 2 x 10^{-5} M PDA in the pH range 4.24 to 9.24. At pH 9.24 the spectrum is that of the free PDA^{2-} anion, which means that the V^V is uncomplexed, and present as the HVO_4^{2-} anion at that pH, as shown from species distribution diagrams generated using HySS.[58] The spectra changes as the pH is lowered, showing peaks typical of PDA complexes with metal ions as one approaches pH 4.24, consistent with the formation of $[VO_2(PDA)]$. Analysis of the spectral changes as was done in Figure 3a, combined with modeling of the V^V species present in solution using equilibrium constants (Table 3) for speciation of vanadate species present in solution[22] yields log K_1 = 7.3 for the formation of the $[VO_2(PDA)]^-$ complex according to equation 3:

$$VO_2^+ + PDA^{2-} \leftrightarrows [VO_2(PDA)]^- \quad (3)$$

The complex polymeric species formed by vanadate in solution between pH 3 and 9 dissociate into monomers below a total concentration of V^V species of 10^{-4} M, as indicated using constants available in the literature[22] and the modeling program HySS,[58] and so are not of any further concern here. HySS was used to model the species distribution diagram for vanadate and PDA as seen in Figure 4b.

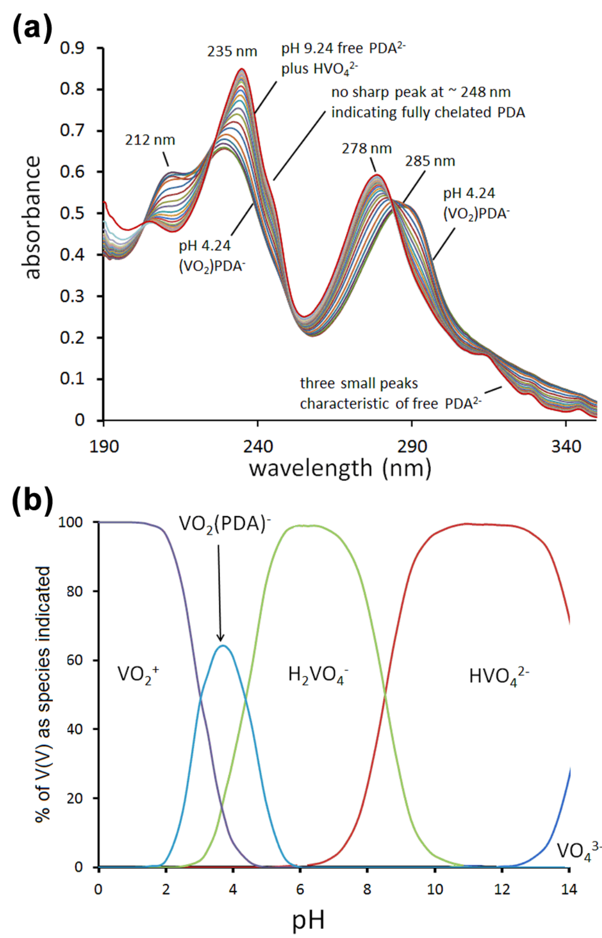

Figure 4. (a) Spectra of 2 x 10^{-5} M PDA 1:1 with 2 x 10^{-5} M Na_3VO_4 in the pH range 4.24 to 9.24 at 25 °C. The peaks at 235 and 278 nm, as well as the three small peaks between 310 and 350 nm, are characteristic of the free PDA^{2-} anion, while peaks near 212 and 285 nm are typical of complexes of metal ions with PDA, indicating the formation of the $[VO_2(PDA)]^-$ complex at lower pH. Note the lack of a sharp small peak near 248 nm (compare with $[UO_2(PDA)]$ in Figure 3b) which would be indicative of formation of a fully chelated PDA complex with the metal ion.[25-27] (b) Species distribution diagram calculated using HySS[58] for 2.0 x 10^{-5} M PDA and 2.0 x 10^{-5} M Na_3VO_4, as a function of pH at ionic strength zero. The diagram was calculated using formation constants relating to vanadate speciation given in ref. 21, relevant ones of which are given in Table 3, and log K_1 = 7.3 determined here for the $[VO_2(PDA)]^-$ complex. Note the existence of the $[VO_2(PDA)]^-$ complex in the pH range 2-6.

Table 3. Equilibrium Constants for the VO_2^+/PDA Complex, Together with Literature Constants for the V^V Solution Species Used in This Paper for Modeling Vanadate Solution Species, All at 25 °C and Ionic Strength (μ) = 0[22, 59-61]

equilibrium	log *K*	ref.
$VO_2^+ + PDA^{2-} \leftrightarrows VO_2(PDA)^-$	7.3(1)	this work
$VO_4^{3-} + H^+ \leftrightarrows HVO_4^{2-}$	14.3	22
$HVO_4^{2-} + H^+ \leftrightarrows H_2VO_4^-$	8.55	22
$H_2VO_4^- + 2H^+ \leftrightarrows VO_2^+ + 2H_2O$	7.3	22
$VO_2^+ + CO_3^{2-} \leftrightarrows VO_2(CO_3)^-$	6.5*	this work

*Estimated as described in the text from the LFER in Figure S1 of the Supporting Information.

Vanadyl(IV)/PDA complexes. The spectra recorded for the 10:1 VO^{2+}/PDA system with 2.0 x 10^{-4} M VO^{2+} and 2 x 10^{-5} M PDA between pH 1.91 and 4.66 are seen in Figure 5. The equilibrium being observed can most reasonably be assigned to equation 4:

$$VO^{2+} + PDAH_2 \leftrightarrows [VO(PDA)] + 2H^+ \qquad (4)$$

The pH_{50} value of 2.12 for equilibrium 3 allows one to fit log K_1 = 7.4(1) (Table 4) for the VO^{2+}/PDA complex.

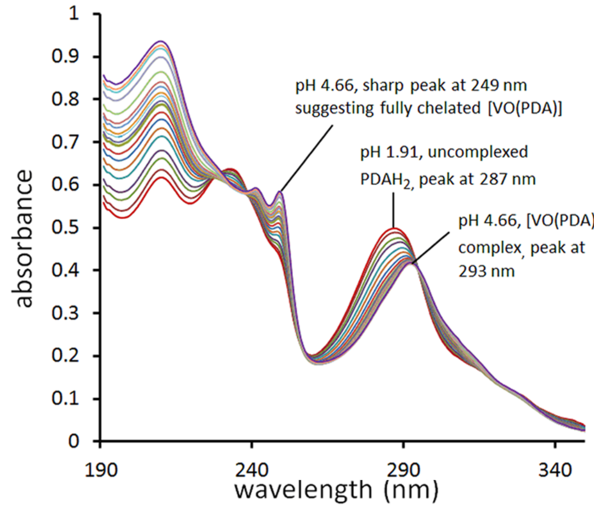

Figure 5. Titration of 2 x 10^{-4} M VO^{2+} and 2 x 10^{-5} M PDA (10:1 VO^{2+}:PDA) between pH 1.91 and 4.66 at 25 °C and ionic strength zero. Note the sharp peak at 249 nm suggesting the VO^{2+} forms a complex with PDA with three fully formed chelate rings.

Table 4. Equilibrium Constants for the VO^{2+}/PDA Complex, Together with Literature Constants for the Associated V^{IV} Hydroxo Species, All at 25 °C and Ionic Strength (μ) = 0[22, 59-61]

equilibrium	log *K*	ref.
$VO^{2+} + PDA^{2-} \leftrightarrows VO(PDA)$	7.4(1)	this work
$VO^{2+} + OH^- \leftrightarrows VO(OH)^+$	8.3	22
$VO^{2+} + 2OH^- \leftrightarrows VO(OH)_2(s)$	-22.1	22
$VO^{2+} + CO_3^{2-} \leftrightarrows VO(CO_3)$	8.1*	this work

*Estimated as described in the text from the LFER in Figure S1 of the Supporting Information.

Comparison of Binding Strength.

The value of log K_1 of 16.5 obtained for the UO_2^{2+}/PDA complex is very high for a dicarboxylic acid, and is exceeded for UO_2^{2+} only by the log K_1 values reported by Shinkai et al.[20] for complex ligands of the L_1 type (Figure 1). It can be compared with log K_1 = 11.4 for EDDA with UO_2^{2+}.[63] Like PDA, EDDA has an N_2O_2 donor set, with the O donors being carboxylates. The extra stability of the PDA complex thus derives from the high level of preorganization of the PDA ligand compared to the more flexible EDDA. Such stabilization of the PDA relative to the EDDA complex is typical, except for very small metal ions such as Cu^{II}, where log K_1 for EDDA is 16.2 and for PDA is 12.8.[25-27] The value of log K_1 = 5.2 for the binding of an OH^- to the PDA complex (Table 2) means that the complex between UO_2^{2+} and PDA is further stabilized, and the uranyl ion remains bound to PDA to a high pH of over 11, as seen in Figure 3d. The changes in the fluorescence spectrum of the UO_2^{2+}/PDA system as a function of pH seen in Figure 3b are of some interest. As the pH is lowered below 12.3, the intensity of the fluorescence due to free PDA^{2-} drops as the $[UO_2(PDA)(OH)]^-$ complex is formed. Below pH 10 as the $[UO_2(PDA)(H_2O)]$ complex is formed, assuming that protonation of the bound OH^- produces a bound H_2O, one sees that the fluorescence in the range 330 to 430 nm falls to almost zero. The latter drop in intensity is accompanied by the appearance of fluorescence peaks in the range 480-530 nm. The latter peaks resemble those formed by UO_2^{2+} hydroxy complexes in the pH range 5-9,[10] but the peaks in Figure 3b do not resemble those of UO_2^{2+}/hydroxyl complexes in details such as overall shape or position of the sharp peaks normally attributed to coupled vibrations. We thus propose that the peaks that appear in the wavelength range 480 to 530 nm in Figure 3b are due to transitions within the UO_2^{2+} bound to PDA. The progressive quenching of the fluorescence due to the PDA in the 330 to 430 nm range as it becomes bound to UO_2^{2+} may be due to the fluorescence-quenching ability of the stretching vibrations of O-H bonds[64] from first an OH^-, and then an H_2O, coordinated to the UO_2^{2+}.

It is clear from the high log K_1 of 16.5 for the $[UO_2(PDA)]$ complex that UO_2^{2+} should be bound very selectively relative to the $[VO_2(PDA)]^-$ and $[VO(PDA)]$ complexes, both with log K_1 values of 7.3 and 7.4, respectively. This is particularly important, as PDA is much more selective for uranyl over vanadium than glutarimidedioxime, a cyclic imidedioxime ligand, which is reputedly responsible for the extraction of uranium from seawater using the current generation of amidoxime-derived sorbents.[11]

Structures and Stabilities of UO_2^{2+}, VO_2^+, and VO^{2+} Complexes with PDA Ligand from Theoretical Calculations.

Density functional theory (DFT) calculations at the M06/SSC/6-311++G** level of theory were performed to elucidate the optimal coordination modes and geometries of uranyl, vanadate(V), and vanadyl(IV) complexes with PDA. The most stable structures of the complexes are shown in Figure 6. Consistent with previous single-crystal X-ray diffraction data,[26] our calculations show that the PDA anion is bound to the uranyl cation in a tetradentate fashion through both nitrogen atoms at an average distance of 2.56 Å and through two carboxylate oxygen atoms at an average distance of 2.34 Å (Figure 6a). It is noteworthy that the PDA ligand in the UO_2^{2+}/PDA complex is almost exactly planar, with the uranium atom lying in the plane of the ligand, which suggests that the PDA is highly preorganized for uranyl complexation and tends to coordinate to UO_2^{2+} in a low-strain manner. While X-ray diffraction studies[26] of UO_2^{2+}/PDA indicate that the uranyl ion is five-coordinate, the preferred coordination number for the corresponding species in water has not yet been identified. Thus, we used DFT calculations (M06 and SMD) to determine the most stable coordination environment in aqueous solution. The free energy change, ΔG_{aq}, calculated for the equilibrium shown by eq (a):

$$[UO_2(PDA)(H_2O)] + H_2O \leftrightarrows [UO_2(PDA)(H_2O)_2], \quad \Delta G_{aq} = +4.52 \text{ kcal/mol} \qquad (a)$$

suggests that the five-coordinate structure (Figure 6a) is more thermodynamically stable than the six-coordinate UO_2^{2+}/PDA with two water molecules bound to UO_2^{2+}.

The structure of the VO_2^+ complex of PDA (Figure 6b) further confirms our expectations that vanadium (V) would be too small to accommodate simultaneous binding of all four donor atoms of PDA. Our initial structure for a DFT optimization, consisting of the VO_2^+ bonded to all four donor atoms of PDA and one water molecule, refined to a structure with only three-coordinating PDA (Figure 6b), with one carboxylate group left noncoordinated and hydrogen-bonded to a water on the VO_2^+. Although our calculations for the VO_2^+/PDA complex without any additional water molecules converge to a local minimum with four-coordinating PDA, the formation of $[VO_2(PDA)]^-$ is less thermodynamically favorable compared to the $[VO_2(PDA)(H_2O)]^-$ complex, as follows from the negative ΔG_{aq} value for eq (b):

$$[VO_2(PDA)]^- + H_2O \leftrightarrows [VO_2(PDA)(H_2O)]^-, \quad \Delta G_{aq} = -5.33 \text{ kcal/mol} \qquad (b)$$

In contrast to vanadium(V), vanadium(IV) is able to coordinate with all four donor atoms of PDA simultaneously. The five-coordinate vanadium(IV) complex, $[VO(PDA)]$, in Figure 6c was found to be ~10 kcal/mol more stable than the corresponding six-coordinate $[VO(PDA)(H_2O)]$ complex with an additional water bonded to the vanadium metal center:

$[VO(PDA)] + H_2O \leftrightarrows [VO(PDA)(H_2O)]$, ΔG_{aq} = +10.42 kcal/mol (c)

However, thorough examination of the [VO(PDA)] structure indicates that the ionic radius of vanadium(IV) is still small for an ideal coordination in the cleft of PDA, because the VO^{2+} cation induces deviation from planarity and distortions in the PDA ligand upon binding (Figure 6c). Our calculations at the M06/SSC/6-311++G** level of theory show that the PDA ligand strain energy upon binding with VO^{2+} is as much as 34.78 kcal/mol higher than the strain energy associated with negligible structural changes of PDA when binding the UO_2^{2+} cation.

The theoretically obtained structures of the UO_2^{2+}, VO_2^{+}, and VO^{2+} complexes with PDA (Figure 6) are in agreement with their experimental electronic spectra. The spectra of UO_2^{2+}/PDA (Figure 3a) and VO^{2+}/PDA (Figure 5) show a sharp band at 247 nm, indicating all four donor atoms of PDA to be coordinated to the corresponding oxycations. In contrast, no band is present at 247 nm in the spectrum of the VO_2^{+} species (Figure 4), which is unlikely to contact all donor atoms of the PDA ligand simultaneously.

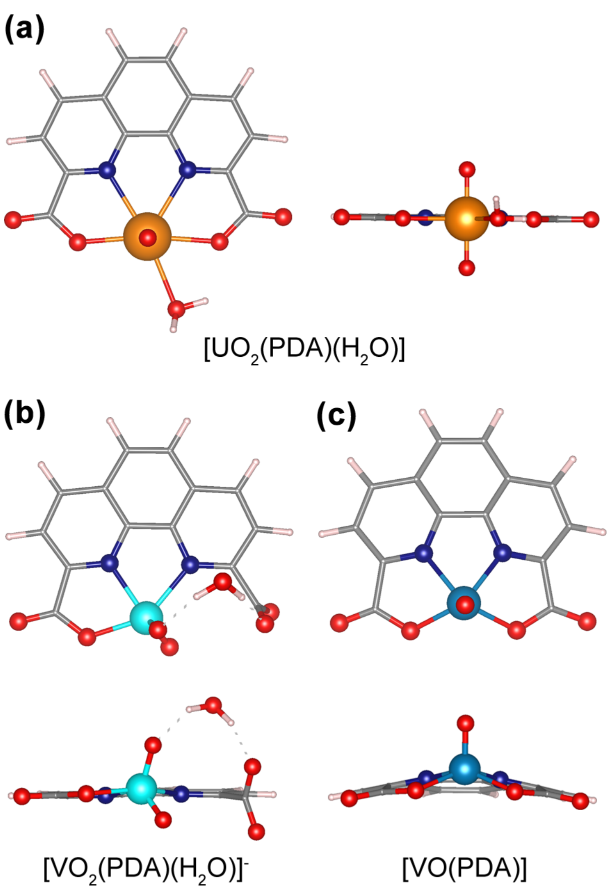

Figure 6. Top and side views of the fully optimized geometries (M06/SSC/6-311++G(d,p)) of aqueous 1:1 (a) UO_2^{2+}/PDA, (b) VO_2^{+}/PDA, and (c) VO^{2+}/PDA complexes. Color legend: O, red; N, navy blue; C, grey; H, white; V(V), turquoise; V(IV), blue; U, orange.

Having established the most stable forms of the UO_2^{2+}, VO_2^{+}, and VO^{2+} complexes with PDA, we can now computationally assess their individual stability constant (log K_1) values using our DFT-based methodology for predicting stability constants of uranyl[47,48] and vanadium[49] complexes. The results given in Table 5 verify that our computational protocol provides very accurate estimates of the log K_1 values (with the maximum absolute error of 0.5 log units) for 1:1 $[UO_2(PDA)(H_2O)]$, $[VO_2(PDA)(H_2O)]^-$, and [VO(PDA)] complexes. Mutual consistency of experimental and theoretically predicted stability constant values of the PDA complexes further confirms the validity of the presented log K_1 data.

Table 5. Experimental and theoretically calculated log K_1 Values for Uranyl, Dioxovanadium(V), and Oxovanadium(IV) Complexes with PDA Ligand

complex	log K_1 experimental[a]	log K_1 calculated[b]	abs. error
$[UO_2(PDA)(H_2O)]$	16.5	16.0	0.5
$[VO_2(PDA)(H_2O)]^-$	7.3	7.2	0.1
[VO(PDA)]	7.4	7.5	0.1

[a]Determined in this work.
[b]Calculated using the methodology described in refs. 47,48 (UO_2^{2+} complexes) and ref.49 (VO_2^{+} and VO^{2+} complexes).

As one may see from Table 5, the log K_1 value of $[UO_2(PDA)(H_2O)]$ is significantly greater in magnitude than the log K_1 values of the vanadium complexes with PDA. Therefore, our results indicate that the PDA ligand is better organized for binding with large UO_2^{2+} than with small VO_2^{+} and VO^{2+} cations. In spite of the fact that VO^{2+} is able to coordinate to all four donor atoms of PDA, this induces high ligand strain resulting in a low log K_1 value, which is similar to that of the VO_2^{+}/PDA complex. This phenomenon can also be rationalized within the framework of natural bond orbital (NBO) analysis. NBO reveals that the chemical bonding between metal oxycations (M = UO_2^{2+}, VO_2^{+}, or VO^{2+}) and PDA has an essentially dative character, i.e., the occupied electron lone pairs of the anionic carboxylates O as well as the lone pairs of the phenanthroline N donor atoms enter into the vacant valence orbitals of M to form coordinative σ bonds. The main results with respect to the strength of $LP_O \rightarrow n^*_M$ (carboxylate) and $LP_N \rightarrow n^*_M$ (phenanthroline) donor-acceptor NBO interactions associated with the donation of electron density from carboxylate and phenanthroline functional groups of the PDA ligand to M are summarized in Table 6. The donor-acceptor interactions between PDA and UO_2^{2+} were found to be substantially stronger than those between PDA and VO^{2+}. As indicated in Table 6, second-order perturbation theory[50] suggests that the strength of the $LP_O \rightarrow n^*_M$ and $LP_N \rightarrow n^*_M$ interactions is ~174 kcal/mol and ~22 kcal/mol greater for the UO_2^{2+}/PDA than for the VO^{2+}/PDA complex. This is caused by the high levels of PDA preorganization that sustains a greater overlap between the O p- and N p-type lone pairs of the ligand and the vacant f-orbitals of UO_2^{2+} than VO^{2+} d-orbitals, resulting in stronger M←:O and M←:N dative bonds in the [UO_2(PDA)(H_2O)] complex than is observed in [VO(PDA)]. The [VO_2(PDA)(H_2O)]$^-$ complex is stabilized through $LP_O \rightarrow n^*_M$ and $LP_N \rightarrow n^*_M$ interactions by only 87.7 and 67.1 kcal/mol, respectively, because VO_2^+ does not bond to all four donor atoms of PDA (see Figure 6b).

Table 6. Leading donor-acceptor natural bond orbital interactions and their second-order stabilization energies $E^{(2)}$ (kcal/mol) for UO_2^{2+}, VO_2^+, and VO^{2+} complexes with PDA

complex	donor NBO → acceptor* NBO[a]	
	$LP_O \rightarrow n^*_M$ (carboxylate)	$LP_N \rightarrow n^*_M$ (phenanthroline)
[UO_2(PDA)(H_2O)]	385.7	155.6
[VO_2(PDA)(H_2O)]$^-$	87.7	67.1
[VO(PDA)]	211.2	133.5

[a]The starred and unstarred labels correspond to Lewis (donor) and non-Lewis (acceptor) NBOs, respectively. LP denotes an occupied lone pair; n* denotes vacant metal orbitals. M can be UO_2^{2+}, VO_2^+, or VO^{2+}.

Implications for the Selective Recovery of Uranium from Seawater.

In seawater, one has to take into account the carbonate complexes and the relatively high concentration of carbonate of 2.5 x 10^{-3} M. Stability constant, log K_1, values for the carbonate complexes of UO_2^{2+} are available,[21] but have not been reported for the VO_2^+ and VO^{2+} complexes. We have constructed an LFER (Linear free energy) relationship of log K_1 for VO_2^+ and VO^{2+} complexes with ligands containing negative oxygen donors (e.g. formate, acetate, oxalate, malonate, salicylate, catecholate) versus log K_1 with the corresponding Cu(II) complexes, as seen in Figure S1 of the Supporting Information. The reasonably good LFER yields the estimates for log K_1 for the carbonate complexes of VO_2^+ and VO^{2+} given in Tables 3 and 4, respectively, from the reported value of log K_1 = 6.77 for the Cu^{II} carbonate complex.[22] A species distribution diagram was constructed by incorporating the log K_1 values for the carbonate complexes of UO_2^{2+}, VO_2^+, and VO^{2+}, together with all the hydrolysis constants known for these metal ions[22,59-61] as well as the log K_1 values for the PDA complexes determined here (Figures 3d and 4b). The inclusion of carbonate complexes made little difference to the species distribution diagram for VO_2^+ shown in Figure 4b, so that even without the inclusion of competing UO_2^{2+}, the VO_2^+ cation forms no complexes with PDA at pH 8. These are completely suppressed at this pH by the formation of the very stable $H_2VO_4^-$ anion. Experimentation with the VO^{2+}/PDA system shows that with the inclusion of carbonate at a relatively high concentration of 2.5 x 10^{-3} M as found in seawater, the [VO(PDA)] complex is largely suppressed. To obtain a model that realistically reflects the UO_2^{2+} speciation in the presence of the PDA ligand under seawater conditions, the stability constants of the ternary (Ca^{2+}/Mg^{2+})-UO_2^{2+}-CO_3^{2-} complexes must also be included in the simulations.[65] As one may see from Figure 7, even in the presence of 0.001 M PDA (very small concentration) at the seawater pH = 8.3, more than 90% UO_2^{2+} is complexed by PDA (65% [UO_2(PDA)], 30% [UO_2(PDA)OH]$^-$), while [$UO_2(CO_3)_3Ca_2$] and [$UO_2(CO_3)_3Mg$]$^{2-}$ only account for 5% UO_2^{2+}. One can thus conclude with confidence that that the PDA ligand would exclusively bind UO_2^{2+} and effectively compete with the formation of carbonate complexes under seawater conditions. It is worth mentioning that the low hydrophilicity of the PDA aromatic backbone may be the major challenge associated with the successful operation of the potential PDA-based polymer adsorbents. However, functionalizing the phen backbone with amines or alcohols can be sufficient to improve the solubility of PDA while increasing its electron donation properties and thus UO_2^{2+}–PDA bond strength. Hence, we expect that ion-exchange materials based on a PDA functional group would be highly efficient and selective for UO_2^{2+} over the vanadium species present in seawater.

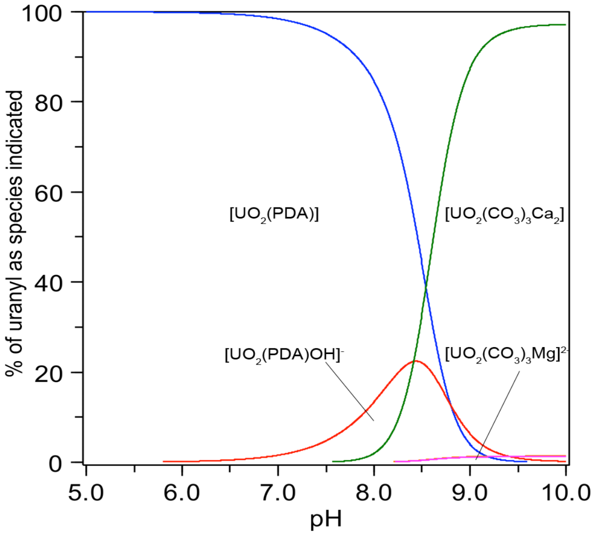

Figure 7. UO_2^{2+} speciation in seawater conditions calculated using the values of log K_1 from Table 2. The values for the formation of the aqueous species (Ca^{2+}/Mg^{2+})-UO_2^{2+}-CO_3^{2-} are taken from Endrizzi and Rao.[65] $C(CO_3^{2-})$ = 0.0025 M, $C(UO_2^{2+})$ = 1.4 x 10^{-8} M, $C(Ca^{2+})$ = 0.010 M, $C(Mg^{2+})$= 0.053 M, $C(PDA^{2-})$ = 0.001 M.

CONCLUSIONS

In this work, we assessed the potential of the PDA (1,10-phenanthroline-2,9-dicarboxylic acid) ligand for the extraction of uranium from seawater by using a combination of fluorescence and absorbance studies, along with density functional theory (DFT) calculations. It was found that PDA is highly preorganized for uranyl complexation and tends to coordinate to UO_2^{2+} in a low-strain manner. The stability constant value (log K_1) of 16.5 obtained for the UO_2^{2+}/PDA complex is high compared to uranyl complexes with other dicarboxylic and representative amidoxime ligands, suggesting that PDA can form strong UO_2^{2+} complexes and effectively compete with carbonate ions for the complexation of UO_2^{2+} at the pH of seawater and in the presence of vanadium species. Therefore, ligand preorganization plays a significant role in the enhanced uranyl binding affinity and selectivity.

An important result from our studies of PDA is that it has several advantages over a glutarimidedioxime ligand, which is reputedly responsible for the extraction of uranium from seawater using the current state of the art amidoxime-based adsorbents.[11] For instance, glutarimidedioxime is highly unstable under strongly alkaline or acidic stripping conditions and has the drawback of low selectivity for uranium over vanadium cations.[16] In contrast, PDA shows no sign of decomposition on standing in HNO_3 or NaOH for three months. Moreover, PDA exhibits strong size-based selectivity in that the determined log K_1 values of the PDA complexes of the vanadium ions are low (log K_1 = 7.3 (VO_2^+) and 7.4 (VO^{2+})) and the ligand is expected to be stable during UO_2^{2+} stripping from the adsorbent, which should occur in basic solution of pH ~ 12. DFT calculations suggest that the vanadium cations are too small for ideal coordination in the cleft of PDA: while the vanadium(IV) adapts to this by inducing deviation from planarity and notable distortions in the structure of the PDA ligand, vanadium(V) is not able to coordinate with all four donor atoms of PDA simultaneously, as indicated by the absence of the sharp band at 247 nm in the electronic spectrum of the VO_2^+/PDA complex. Hence, the structural preorganization helps PDA achieve higher binding affinity for UO_2^{2+} over the VO_2^+ and VO^{2+} ions, which is due to the strong dative interactions between UO_2^{2+} and functional groups of the ligand, promoting stronger coordination with the uranyl cation, as suggested by the NBO analysis. Overall, due to its high chemical stability and selectivity for uranyl, PDA is a very promising candidate for the development of novel adsorbent materials for the selective extraction of uranium from seawater.

ASSOCIATED CONTENT

Supporting Information. Linear Free Energy Relationship (LFER) of log K_1 values for ligands with negative oxygen donors with the VO^{2+} cation or the VO_2^+ cation versus log K_1 for Cu(II), sample Gaussian 09 input file, Cartesian coordinates of the PDA ligand and metal-ligand complexes obtained with M06 density functional. This material is available free of charge via the Internet at http://pubs.acs.org.

AUTHOR INFORMATION

Corresponding Author

*(R.D.H.) E-mail: hancockr@uncw.edu.

*(V.S.B.) E-mail: bryantsevv@ornl.gov.

Funding

This work was sponsored by the US Department of Energy, Office of Nuclear Energy, under Contract DE-AC05-00OR22725 with Oak Ridge National Laboratory, managed by UT-Battelle, LLC.

Author Contributions

#M. A. Lashley and A. S. Ivanov contributed equally.

ACKNOWLEDGMENT

The authors thank Dr. Carter W. Abney (ORNL) for critically reading the manuscript and offering helpful suggestions. This research used resources of the National Energy Research Scientific Computing Center, a DOE Office of Science User Facility supported by the Office of Science of the U.S. Department of Energy under Contract No. DE-AC02-05CH11231.

REFERENCES

(1) Sholl, D. S.; Lively, R. P. Seven Chemical Separations to Change the World. *Nature* **2016**, *532*, 435.

(2) Rao, L. "Recent International R&D Activities in the Extraction of Uranium from Seawater," Lawrence Berkeley National Laboratory, 5 Jan 2011.

(3) "Analysis of the Uranium Supply to 2050," International Atomic Energy Agency, STI/PUB/1104, May 2001.

(4) Kanno, M. Present Status of Study on Extraction of Uranium from Sea Water. *J. Nucl. Sci. Technol.* **1984**, *21*, 1.

(5) Seko, N.; Tamada, M.; Yoshii, F. Current Status of Adsorbent for Metal Ions with Radiation Grafting and Crosslinking Techniques. *Nucl. Instrum. Meth. Physics Res.* **2005**, *B236*, 21.

(6) Kim, J.; Tsouris, C.; Mayes, R. T.; Oyola, Y.; Saito, T.; Janke, C. J.; Dai, S.; Schneider, E.; Sachde, D. Recovery of Uranium from Seawater: A Review of Current Status and Future Research Needs. *Sep. Sci. Technol*. **2013**, *48*, 367.

(7) Seko, N.; Katakai, A.; Hasegawa, S.; Tamada, M.; Kasai, N.; Takeda, H.; Sugo, T.; Saito, K. Aquaculture of Uranium in Seawater by a Fabric-Adsorbent Submerged System. *Nucl. Technol*. **2003**, *144*, 274.

(8) Chester, R.; Jickells, T. D. (2012). *Marine Geochemistry*. 3rd Edition, Wiley-Blackwell Publishing, New York, 2012.

(9) a) Tabushi, I.; Kobuke, Y.; Nishiya, T. Extraction of Uranium from Seawater by Polymer-bound Macrocyclic Hexaketone. *Nature* **1979**, *280*, 665; b) Tamada, M.; Seko, N.; Kasai, N.; Shimizu, T. Cost Estimation of Uranium Recovery from Seawater with System of Braid Type Adsorbent. *Trans. At. Energy Soc. Japan*, **2006**, 5, 358.

(10) Lashley, M. A.; Mehio, N.; Nugent, J. W.; Holguin,E.; Do-Thanh,C. L.; Bryantsev, V. S.; Dai, S.; Hancock, R. D. Amidoximes as Ligand Functionalities for Braided Polymeric Materials for the Recovery of Uranium from Seawater. *Polyhedron* **2016**, *109*, 81.

(11) a) Tian, G.; Teat, S. J.; Zhang, Z.; Rao, L. Sequestering Uranium from Seawater: Binding Strength and Modes of Uranyl Complexes with Glutarimidedioxime. *Dalton Trans.* **2012**, *41*, 11579; b) Tian, G.; Teat, S. J.; Rao, L. Thermodynamic Studies of U (VI) Complexation with Glutardiamidoxime for Sequestration of Uranium from Seawater. *Dalton Trans*. **2013**, *42*, 5690; c) Sun, X.; Tian, G.; Xu, C.; Rao, L.; Vukovic, S.; Kang, S.; Hay, B. P. Quantifying the Binding Strength of U (VI) with Phthalimidedioxime in Comparison with Glutarimidedioxime. *Dalton Trans*. **2014**, *43*, 551.

(12) a) Sun, X.; Xu, C.; Tian, G.; Rao, L. Complexation of Glutarimidedioxime with Fe (III), Cu (II), Pb (II), and Ni (II), the Competing Ions for the Sequestration of U (VI) from Seawater. *Dalton Trans.*, **2013**, *42*, 14621; b) Kim, J.; Tsouris, C.; Oyola, Y.; Janke, C. J.; Mayes, R. T.; Dai, S.; Gill, G.; Kuo, L. J.; Wood, J.; Choe, K. Y.; Schneider, E. Uptake of Uranium from Seawater by Amidoxime-Based Polymeric Adsorbent: Field Experiments, Modeling, and Updated Economic Assessment. *Ind. Eng. Chem. Res.*, **2014**, *53*, 6076.

(13) Wang, D.; Wilhelmy, S. A. S. Vanadium Speciation and Cycling in Coastal Waters. *Mar. Chem*. **2009**, *117*, 52.

(14) Jeandel, C.; Caisso, M.; Minster, J.F. Vanadium Behaviour in the Global Ocean and in the Mediterranean Sea. *Mar. Chem*. **1987**, *21*, 21.

(15) Wehrli, B.; Stumm, W. Vanadyl in Natural Waters: Adsorption and Hydrolysis Promote Oxygenation. *Cosmochim. Acta* **1989**, *53*, 69.

(16) a) Suzuki, T.; Saito, K.; Sugo, T.; Ogura, H.; Oguma, K. Fractional Elution and Determination of Uranium and Vanadium Adsorbed on Amidoxime Fiber from Seawater. *Anal. Sci.*, **2000**, *16*, 429; b) Mehio, N.; Johnson, J. C.; Dai, S.; Bryantsev, V. S. Theoretical Study of the Coordination Behavior of Formate and Formamidoximate with Dioxovanadium (v) Cation: Implications for Selectivity Towards Uranyl. *Phys. Chem. Chem. Phys.*, **2015**, *17*, 31715; c) Mehio, N.; Ivanov, A. S.; Ladshaw, A. P.; Dai, S., Bryantsev, V. S. Theoretical Study of Oxovanadium (IV) Complexation with Formamidoximate: Implications for the Design of Uranyl-Selective Adsorbents. *Ind. Eng. Res. Chem.*, **2015**, 55, 4231; d) Leggett, C. J.; Parker, B. F.; Teat, S. J.; Zhang, Z.; Dau, P. D.; Lukens, W. W.; Peterson, S. M.; Cardenas, A. J. P.; Warner, M. G.; Gibson, J. K.; Arnold, J.; Rao, L. Structural and Spectroscopic Studies of a Rare Non-Oxido V (v) Complex Crystallized from Aqueous Solution. *Chem. Sci.* **2016**, *7*, 2775.

(17) Kawai, T.; Saito, K.; Sugita, K.; Kawakami, T.; Kanno, J.; Katakai, A.; Seko, N.; Sugo, T. Preparation of Hydrophilic Amidoxime Fibers by Cografting Acrylonitrile and Methacrylic Acid from an Optimized Monomer Composition. *Rad. Phys. Chem.* **2000**, *59*, 405.

(18) Cram, D. J.; Cram, J. M. Design of Complexes Between Synthetic Hosts and Organic Guests. *Acc. Chem. Res.* **1978**, *11*, 49.

(19) a) Wilson, A. M.; Bailey, P. J.; Tasker, P. A.; Turkington, J. R.; Grant, R. A.; Love, J. B. Solvent Extraction: the Coordination Chemistry Behind Extractive Metallurgy. *Chem. Soc. Rev.* **2014**, *43*, 123.; b) Izatt, R. M.; Izatt, S. R.; Bruening, R. L.; Izatt, N. E.; Moyer, B. A. Challenges to Achievement of Metal Sustainability in our High-Tech Society. *Chem. Soc. Rev.* **2014**, *43*, 2451.

(20) Shinkai, S.; Koreishi, H.; Ueda, K.; Arimura, T.; Manabe, O. Molecular Design of Calixarene-Based Uranophiles which Exhibit Remarkably High Stability and Selectivity. *J. Am. Chem. Soc.*, **1987**, *109*, 6371.

(21) Thuéry, P.; Nierlich, M. Crystal Structure of a Uranyl/p-tert-Butylcalix [5] Arene Complex. *J. Inclusion Phenom. Mol. Recognit. Chem.*, **1997**, *27*, 13.

(22) Martell, A. E.; Smith, R. M. *Critical Stability Constant Database, 46*, National Institute of Science and Technology (NIST): Gaithersburg, MD, USA, 2003.

(23) Beer, S.; Berryman, O. B.; Ajami, D.; Rebek Jr, J. Encapsulation of the Uranyl Dication. *Chem. Sci.*, **2010**, *1*, 43.

(24) Zhou, L.; Bosscher, M.; Zhang, C.; Ozcubukcu, S.; Zhang, L.; Zhang, W.; Li, C. J.; Liu, J.; Jensen, M. P.; Lai, L.; He, C. A Protein Engineered to Bind Uranyl Selectively and with Femtomolar Affinity. *Nat. Chem.* **2014**, *6*, 236.

(25) Melton, D. L.; VanDerveer, D. G.; Hancock, R. D. Complexes of Greatly Enhanced Thermodynamic Stability and Metal Ion Size-Based Selectivity, Formed by the Highly Preorganized Non-Macrocyclic Ligand 1, 10-Phenanthroline-2, 9-Dicarboxylic Acid. A Thermodynamic and Crystallographic study. *Inorg. Chem.*, **2006**, *45*, 9306.

(26) Dean, N. E.; Hancock, R. D.; Cahill, C. L.; Frisch, M. Affinity of the Highly Preorganized Ligand PDA (1, 10-Phenanthroline-2, 9-Dicarboxylic acid) for Large Metal Ions of Higher Charge. A Crystallographic and Thermodynamic Study of PDA Complexes of Thorium (IV) and the Uranyl (VI) Ion. *Inorg. Chem.*, **2008**, *47*, 2000.

(27) Williams, N. J.; Dean, N. E.; VanDerveer, D. G.; Luckay, R. C.; Hancock, R. D. Strong Metal Ion Size Based Selectivity of the Highly Preorganized Ligand PDA (1, 10-Phenanthroline-2, 9-Dicarboxylic Acid) with Trivalent Metal Ions. A Crystallographic, Fluorometric, and Thermodynamic Study. *Inorg. Chem.,* **2009**, *48*, 7853.
(28) Hancock, R. D. Chelate Ring Size and Metal Ion Selection. The Basis of Selectivity for Metal Ions in Open-Chain Ligands and macrocycles. *J. Chem. Ed*. **1992**, *69*, 615.
(29) Hancock, R. D.; Martell, A. E. Ligand Design for Selective Complexation of Metal Ions in Aqueous Solution. *Chem. Rev*. **1989**, *89*, 1875.
(30) Shannon, R. D. Revised Effective Ionic Radii and Systematic Studies of Interatomic Distances in Halides and Chalcogenides. *Acta Cryst*., **1976**, *A32*, 751.
(31) Merrill, D.; Harrington, J. M.; Lee, H.-S.; Hancock, R. D. Unusual Metal Ion Selectivities of the Highly Preorganized Tetradentrate Ligand 1, 10-Phenanthroline-2, 9-Dicarboxamide: A Thermodynamic and Fluorescence Study. *Inorg. Chem.,* **2011**, *50*, 8348.
(32) Merrill, D.; Hancock, R. D. Metal Ion Selectivities of the Highly Preorganized Tetradentate Ligand 1, 10-Phenanthroline-2, 9-Dicarboxamide with Lanthanide (III) Ions and Some Actinide Ions. *Radiochim. Acta* **2011**, *99*, 161.
(33) Gephart III, R. T.; Williams, N. J.; Reibenspies, J. H., De Sousa, A. S.; Hancock, R. D. Metal Ion Complexing Properties of the Highly Preorganized Ligand 2, 9-Bis (Hydroxymethyl)-1, 10-Phenanthroline: A Crystallographic and Thermodynamic Study. *Inorg. Chem.,* **2008**, *47*, 10342.
(34) Gephart III, R. T.; Williams, N. J.; Reibenspies, J. H., De Sousa, A. S.; Hancock, R. D. Complexation of Metal Ions of Higher Charge by the Highly Preorganized Tetradentate Ligand 2, 9-bis (Hydroxymethyl)-1, 10-Phenanthroline. A Crystallographic and Thermodynamic Study. *Inorg. Chem.,* **2009**, *48*, 8201.
(35) Williams, N. J.; Balance, D. G.; Reibenspies, J. H., A. S.; Hancock, R. D. Complexes of the Highly Preorganized Ligand PDALC (2, 9-bis (hydroxymethyl)-1, 10-phenanthroline) with Trivalent Lanthanides. A Thermodynamic and Crystallographic Study. *Inorg. Chim. Acta* **2010**, *363*, 3694.
(36) Cockrell, G. M.; Zhang, G.; VannDerveer, D. G.; Thummel, R. P.; Hancock, R. D. Enhanced Metal Ion Selectivity of 2, 9-di-(pyrid-2-yl)-1, 10-Phenanthroline and Its Use as a Fluorescent Sensor for Cadmium (II). *J. Am. Chem. Soc.*, **2008**, *130*, 1420.
(37) Carolan, A. N.; Cockrell, G. M.; Williams, N. J.; El Ojaimi, M.; VanDerveer, D. G.; Thummel, R. P.; Hancock, R. D. Selectivity of the Highly Preorganized Tetradentate Ligand 2, 9-di (pyrid-2-yl)-1, 10-Phenanthroline for Metal Ions in Aqueous Solution, Including Lanthanide (III) Ions and the Uranyl (VI) Cation. *Inorg. Chem*. **2013**, *52*, 15.
(38) Chandler, C. J.; Deady, L. W.; Reiss, J. A. Synthesis of Some 2, 9-Disubstituted-1, 10-Phenanthrolines. *J. Heterocyclic Chem*. **1981**, *18*, 599.
(39) Billo, E. J. *EXCEL for Chemists*. Wiley VCH: New York, 2001.
(40) Frisch, M. J.; Trucks, G. W.; Schlegel, H. B.; Scuseria, G. E.; Robb, M. A.; Cheeseman, J. R.; Scalmani, G.; Barone, V.; Mennucci, B.; Petersson, G. A.; Nakatsuji, H.; Caricato, M.; Li, X.; Hratchian, H. P.; Izmaylov, A. F.; Bloino, J.; Zheng, G.; Sonnenberg, J. L.; Hada, M.; Ehara, M.; Toyota, K.; Fukuda, R.; Hasegawa, J.; Ishida, M.; Nakajima, T.; Honda, Y.; Kitao, O.; Nakai, H.; Vreven, T.; Montgomery, J. A., Jr.; Peralta, J. E.; Ogliaro, F.; Bearpark, M.; Heyd, J. J.; Brothers, E.; Kudin, K. N.; Staroverov, V. N.; Kobayashi, R.; Normand, J.; Raghavachari, K.; Rendell, A.; Burant, J. C.; Iyengar, S. S.; Tomasi, J.; Cossi, M.; Rega, N.; Millam, M. J.; Klene, M.; Knox, J. E.; Cross, J. B.; Bakken, V.; Adamo, C.; Jaramillo, J.; Gomperts, R.; Stratmann, R. E.; Yazyev, O.; Austin, A. J.; Cammi, R.; Pomelli, C.; Ochterski, J. W.; Martin, R. L.; Morokuma, K.; Zakrzewski, V. G.; Voth, G. A.; Salvador, P.; Dannenberg, J. J.; Dapprich, S.; Daniels, A. D.; Farkas, O.; Foresman, J. B.; Ortiz, J. V.; Cioslowski, J.; Fox, D. J. Gaussian, Inc., Wallingford CT, 2009.
(41) Zhao, Y.; Truhlar, D. G. The M06 Suite of Density functionals for Main Group Thermochemistry, Thermochemical Kinetics, Noncovalent Interactions, Excited States, and Transition Elements: Two New Functionals and Systematic Testing of Four M06-Class Functionals and 12 Other Functionals. *Theor. Chem. Acc.*, **2008**, *120*, 215.
(42) Dolg, M.; Stoll, H.; Preuss, H.; Pitzer, R. M. Relativistic and Correlation Effects for Element 105 (Hahnium, Ha): a Comparative Study of M and MO (M= Nb, Ta, Ha) using Energy-Adjusted ab initio Pseudopotentials. *J. Phys. Chem.*, **1993**, *97*, 5852.
(43) a) Becke, A. D. Density-Functional Thermochemistry. III. The Role of Exact Exchange. *J. Chem. Phys.*, **1993**, *98*, 5648; b) Lee, C.; Yang, W.; Parr, R. G. Development of the Colle-Salvetti Correlation-Energy Formula into a Functional of the Electron Density. *Phys. Rev. B*, **1988**, *37*, 785.
(44) Pitzer, K. S.; Gwinn, W. D. Energy Levels and Thermodynamic Functions for Molecules with Internal Rotation I. Rigid Frame with Attached Tops. *J. Chem. Phys***. 1942**, *10*, 428.
(45) Ayala, P. Y.; Schlegel, H. B. Identification and Treatment of Internal Rotation in Normal Mode Vibrational Analysis. *J. Chem. Phys.* **1998**, *108*, 2314.
(46) Marenich, A. V.; Cramer, C. J.; Truhlar, D. G. Universal Solvation Model Based on Solute Electron Density and on a Continuum Model of the Solvent Defined by the Bulk Dielectric Constant and Atomic Surface Tensions. *J. Phys. Chem. B*, **2009**, *113*, 6378.
(47) Vukovic, S.; Hay, B. P.; Bryantsev, V. S. Predicting Stability Constants for Uranyl Complexes Using Density Functional Theory. *Inorg. Chem.,* **2015**, *54*, 3995.
(48) Mehio, N.; Ivanov, A. S.; Williams, N. J.; Mayes, R. T.; Bryantsev, V. S.; Hancock, R. D.; Dai, S. Quantifying the Binding Strength of Salicylaldoxime–Uranyl Complexes Relative to Competing Salicylaldoxime–Transition Metal Ion Complexes in Aqueous Solution: a Combined Experimental and Computational Study. *Dalton. Trans*., **2016**, *45*, 9051.
(49) Ivanov, A. S.; Bryantsev, V. S. Assessing Ligand Selectivity for Uranium over Vanadium Ions to Aid in the Discovery of Superior Adsorbents for Extraction of $UO2^{2+}$ from Seawater. *Dalton. Trans.,* **2016**, 45, 10744.
(50) Foster, J. P.; Weinhold, F. Natural Hybrid Orbitals. *J. Am. Chem. Soc.*, **1980**, *102*, 7211.
(51) Vyboishchikov, S. F.; Sierraalta, A.; Frenking, G. Topological Analysis of Electron Density Distribution Taken From a Pseudopotential Calculation. *J. Comput. Chem.* **1997**, *18*, 416.
(52) Pantazis, D. A.; Chen, X.-Y.; Landis, C. R.; Neese, F. All-electron Scalar Relativistic Basis Sets for Third-Row Transition Metal Atoms. *J. Chem. Theory Comput.* **2008,** *4,* 908.
(53) Das, S.; Liao, W.-P.; Flicker Byers, M.; Tsouris, C.; Janke, C. J.; Mayes, R. T.; Schneider, E.; Kuo, L.-J.; Wood, J. R.; Gill, G. A.; Dai, S. Alternative Alkaline Conditioning of Amidoxime Based Adsorbent for Uranium Extraction from Seawater. *Ind. Eng. Res. Chem.* **2016,** 55, 4303.
(54) Choi, S.-H.; Nho, Y. C. Adsorption of UO_2^{2+} by Polyethylene Adsorbents with Amidoxime, Carboxyl, and Amidoxime/Carboxyl Group. *Radiat. Phys. Chem.* **2000**, 57, 187.
(55) Wang, C. Z.; Lan, J.-H.; Wu, Q. Y.; Luo, Q.; Zhao, Y. L.; Wang, X. K.; Chai, Z. F.; Shi, W. Q. Theoretical Insights on the Interaction of Uranium with Amidoxime and Carboxyl Groups. *Inorg. Chem.*, **2014**, 53, 9466.
(56) Davies, C. W. *Ion Association*; Butterworths: Washington, DC, 1962.

(57) Ramamoorthy, S.; Santappa, M. Stability Constants of Some Uranyl Complexes. *Bull. Chem. Soc. Japan*, **1968**, *41*, 1330.
(58) Alderighi, L. ; Gans, P.; Ienco, A.; Peters, D.; Sabatini, A.; Vacca, A. Hyperquad Simulation and Speciation (HySS): a Utility Program for the Investigation of Equilibria Involving Soluble and Partially Soluble Species. *Coord. Chem. Rev.* **1999**, *184*, 311.
(59) Grenthe, I.; Drozdzynski, J.; Fujino, T.; Buck, E. C.; Albrecht-Schmitt, T. E.; Wolf, S. F.: *The chemistry of the actinide and transactinide elements*, 3rd ed., Morss, L. R., Edelstein, N. M., Fuger, J. (eds.). Springer: Netherlands, 2006, Vol. 1, pp. 599-601.
(60) Grenthe, I.; Fuger, J.; Konings, R. J. M.; Lemire, R. J.; Muller, A. B.; Nguyen-Trung, C.; Wanner, H. *Chemical Thermodynamics of Uranium*, NEA/OECD, North Holland, 1992.
(61) Guillamont, R.; Fanghänel, T.; Fuger, J.; Grenthe, I.; Palmer, D.; Rand, M.; Neck, V. *Chemical Thermodynamics of Uranium, Neptunium, Plutonium, Americium, and Technetium*, NEA/OECD, North Holland, 2003.
(62) Lakowicz, J. R. Pruinciples of Fluorescence Spectroscopy, 3rd Edition, Springer, New York, 2006.
(63) Palladino, G.; Szabo, G.; Fischer, A.; Grenthe, I. Structure, Equilibrium and Ligand Exchange Dynamics in the Binary and Ternary Dioxouranium (vi)-Ethylenediamine-N, N′-Diacetic Acid-Fluoride System: a Potentiometric, NMR and X-ray Crystallographic Study. *Dalton Trans*. **2006**, *43*, 5176.
(64) Fazekas, Z.; Tomiyasu, H.; Park, I.-L.; Yamamura, T.; Harada, M. *Models in Chemistry*, 135, Akademiai Kiadó, Budapest, 1998.
(65) Endrizzi, F.; Leggett, C. J.; Rao. L. Scientific Basis for Efficient Extraction of Uranium from Seawater. I: Understanding the Chemical Speciation of Uranium under Seawater Conditions. *Ind. Eng. Chem. Res.* **2016**, 55, 4249.

Table of Contents

Synopsis: Using UV/Vis, fluorescence, and quantum chemical methods we report very high selectivity of the PDA (1,10-phenanthroline-2,9-dicarboxylic acid) ligand towards UO_2^{2+} over competing VO_2^{+} and VO^{2+} ions, suggesting that PDA could be used as a new functional group in ion-exchange materials for the selective recovery of uranium from seawater.